31st Annual International Conference of the IEEE EMBS
Minneapolis, Minnesota, USA, September 2-6, 2009

Mathematical Modeling of a Tethered Bilayer Sensor Containing Gramicidin A Ion Channels

Sahar M.Monfared, Vikram Krishnamurthy *Fellow, IEEE*, Bruce Cornell

***Abstract*— This paper considers the mathematical modeling of chemical kinetics and electrical dynamics of a tethered bilayer biosensor, comprising of Gramicidin A (gA) ion channels. The electrical dynamics of the biosensor are modeled by an equivalent second order linear system. The chemical kinetics of the biosensor, which involve the binding of analyte to the receptor sites immobilized on the biosensor surface, are modeled in both the reaction-rate-limited regime, where analyte concentration is constant through out the biosensor flow chamber, and the mass transport influenced region, where the analyte concentration is subject to variations in time and space. Using the theory of Singular Perturbation, we show that the channel conductance varies according to one of three possible modes depending on the analyte concentration present.**

I. Introduction

This paper deals with mathematical modeling of electrical response as well as chemical kinetics of the Ion Channel Switch (ICS) biosensor, developed by our coauthor and published in *Nature*; see also [13], [4], [2]. The ICS biosensor is an example of bilayer lipid membrane based biosensors.The ICS biosensor provides an interesting example of engineering at the nano-scale. It is significant that the functionality of the device depends on approximately 100 lipids, and a single ion channel modulating the flow of billions of ions in a typical sensing event of approximately 5 minutes.

The biological recognition mechanism of the ICS biosensor is the recognition of an antibody or protein by its corresponding antigen or receptor molecule, which translates to changing of the channel conduction. The immunorecognition mechanism of the ICS biosensor, makes it adaptable to a wide range of applications, requiring rapid detection of analytes such as environmental monitoring and general bio-hazard detection.

The main results of this paper are as follows:

1) *Biosensor Operation and Construction:* Section II provides an overview of the construction and operation of the ICS biosensor. For detailed explanation of the construction of this specific biosensor see [13], [11], and [3].
2) *Dynamical Response of Biosensor:* In Section III the electrical dynamics of the ICS biosensor are modeled by an equivalent second order linear system, see [13],[11]. We then formulate the biosensor response to analyte concentration as a two-time scale nonlinear dynamical system in Section IV. The presence of analyte decreases the concentration of the *dimer*s formed in the biosensor, thus decreasing the channel conductance. In order to study the evolution of the channel conductance in response to the introduction of analyte, the chemical kinetics of the biosensor are modeled as a singularly perturbed system, see also [9],[6]. The analyte concentration in the mass transport influenced region of operation of the biosensor is modeled by a partial differential equation subject to a mix of Neumann and Dirchlit boundary conditions in Section IV-B; see [10],[7],[8]. Analysis of the chemical kinetics of the biosensor as a Singularly Perturbed system in Section IV-A, leads to the result that the channel conduction evolves according to three regimes depending on the concentration of the analyte in the system.

II. Constructoin and Operation

The ICS biosensor comprises of a gold electrode, to which a monolayer lipid membrane, containing gramicidin A (gA) ion channels, is attached. Then a second outer mobile monolayer lipid membrane is introduced which also contains gA ion channels. The outer lipid monolayer is mobile and slides against the monolayer tethered to the gold electrode. As the mobile gramicidin ion channels in the outer lipid monolayer diffuse, occasionally a channel in the mobile lipid layer aligns with a channel in the tethered lipid layer and a *dimer* forms. In the presence of an applied potential (typically 100 to 300 mV), ions can travel through the *dimer* towards the gold electrode, thereby establishing a current.

In the construction of the biosensor, specific antibodies that recognize specific analyte molecules are attached to the mobile outer layer channels. If analyte molecules are present in the solution introduced to the biosensor, the arrival of analyte cross-links antibodies attached to the mobile outer layer channels, to those attached to membrane spanning lipid tethers. Due to the low density of tethered channels within the inner membrane, this anchors them distant, on average, from their immobilized inner layer channel partners. Gramicidin *dimer* conduction is thus prevented and the ionic conductance of the membrane decreases. Based on the resulting decrease in current (or equivalently, increase in resistance or decrease in conductance of the membrane), one can detect the presence of analyte. Based on how the

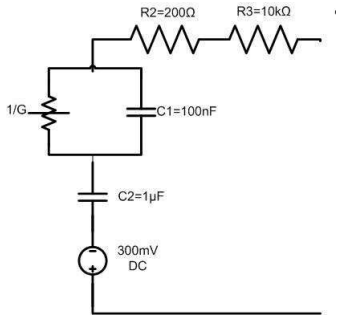

Fig. 1. Equivalent electrical circuit of the ICS biosensor.

conductance decreases with time, one can also estimate the concentration of analyte.

III. ICS Biosensor Modeling

In this section and the next, mathematical models for the electrical response as well as chemical kinetics of the biosensor are constructed.

A. Electrical Dynamics of the Biosensor

The ICS biosensor can be modeled as a biological transistor. Fig.1 illustrates the equivalent circuit of the switch, [13]. The resistor $R = 1/G$ models the biosensor resistance and increases with the presence of analyte. C_1 denotes the capacitance of the membrane and is typically 100nF. R_2 denotes the resistance of the electrolyte – this is typically known to be around 200 Ω. Finally, R_3 denotes the input resistance of the amplifier at the next stage (which is ideally very large). The 300mV bias voltage controls the value of the capacitor C_2. Typically C_2 can change from 1 μF at 300mV to $0.01\mu\text{F}$ at no bias. The biosensor is usually deployed with a 300mV bias. Values of the circuit parameters in Fig. 1, were obtained using channel impedance spectrometer [13].

B. Dynamics of Biosensor Response to Analyte

In this section the ICS biosensor response to null, medium and high analyte concentrations are shown empirically to follow three modes.

Let A denote the unknown concentration of analyte. From detailed experimental analysis of the biosensor and reaction rate dynamics analysis presented in Section IV, it is known that the conductance G of the biosensor evolves according to one of 3 different concentration modes; $\mathcal{M}$:

$$G_{n+1} = f^{\mathcal{M}}(G_n, A^*) + w_n, \tag{1}$$

$$\mathcal{M} = \begin{cases} 1 & A^* = 0 : f^{\mathcal{M}}(G_n, A^*) = G_n \\ 2 & A^*\text{medium} : f^{\mathcal{M}}(G_n, A^*) = \kappa_1 G_n + \kappa_2 \\ 3 & A^*\text{high} : f^{\mathcal{M}}(G_n, A^*) = \kappa_3 G_n + \kappa_4 \end{cases}$$

Here $\kappa_1, \kappa_2, \kappa_3, \kappa_4$ are constants, with $|\kappa_2| < 1$. w_n is a zero mean white Gaussian noise process with small variance and models our uncertainty in the evolution of G. The function $f^{\mathcal{M}}$ models the fact that the admittance G_n of the membrane decreases according to one of 3 distinct modes depending on the concentration A of the analyte. For no analyte present ($\mathcal{M} = 1$), the admittance remains constant. For medium and high analyte concentration ($\mathcal{M} = 2$, $\mathcal{M} = 3$), the conductance decay is exponential with different decay rates.

The response of the ICS biosensor to various concentrations of analyte, Streptavidin, when Biotin is used as a low molecular weight receptor can be found in [2], [13]. Streptavidin-Biotin antigen-antibody interaction has been used through out this text to demonstrate system behavior.

IV. Chemical Dynamics of Biosensor

In this section singular perturbation theory is used to derive equations describing the evolution of the channel conductance as a function of time and analyte concentration. The goal is to mathematically derive equations (1), by analyzing the chemical kinetics of the biosensor.

The reactions involved in the biosensor mainly stem from the binding of the primary species and the secondary species or complexes. The primary species are Analyte, a, of concentration A, binding site γ of concentration Γ, free moving monomeric ion channel δ of concentration Δ, and tethered monomeric ion channel υ of concentration Υ. While the complexes are ν, χ, y and ζ with concentrations, N, X, Y and Z and are formed according to the following equations

$$\begin{array}{lllll} a & + & \gamma \rightleftharpoons^{f_1}_{r_1} \nu, & a+\delta \rightleftharpoons^{f_2}_{r_2} \chi, & \nu+\delta \rightleftharpoons^{f_3}_{r_3} y \\ \delta & + & \upsilon \rightleftharpoons^{f_5}_{r_5} \pi, & a+\pi \rightleftharpoons^{f_6}_{r_6} \zeta & \chi+\delta \rightleftharpoons^{f_7}_{r_7} \zeta \\ \chi & + & \gamma \rightleftharpoons^{f_4}_{r_4} y & & \end{array} \tag{2}$$

where, f_i and r_i for $i = \{1, 2, 3, 4, 5, 6, 7\}$ are respectively the forward and backward reaction rate constants. The forward reaction rate constants, f_i, have units of $(\text{M}^{-1}\text{s}^{-1})$ in case of 3D reactions, and $(\text{cm}^2\text{s}^{-1})$ in case of 2D reactions. The backward reaction rate constants, r_i have units of (s^{-1}).

The total reaction rates can be computed as below,

$$\begin{aligned} R_1 &= f_1 A\Gamma - r_1 N, \quad R_2 = f_2 A\Delta - r_2 X \\ R_3 &= f_3 N\Delta - r_3 Y, \quad R_4 = f_4 X\Gamma - r_4 Y, \\ R_5 &= f_5 \Delta\Upsilon - r_5 \Pi, \quad R_6 = f_6 A\Pi - r_6 Z \\ R_7 &= f_7 X\Upsilon - r_7 Z \end{aligned} \tag{3}$$

The analyte concentration A is generally a function of both space and time.

In a flow cell Diffusion and advection carry analyte molecules to the biomimetic surface where binding occurs according to the chemical kinetics defined in (3). The combination of parameters such as flow rate of the solution containing the analyte, the geometry of the flow cell, the kinetic constants, diffusion coefficient and the density of binding sites distinguishes two operating regimes for the system:(i) reaction-rate-limited kinetics,(ii) mass transport influenced kinetics, [12]. In reaction-rate-limited kinetics regime, mass transport is fast such that any analyte concentration variation

resulting from the chemical kinetics is balanced much faster than it is created, therefore $A(x_1, x_2, x_3, t) = A^*$. Where x_1 denotes the x-axis, x_2 denotes the y-axis and x_3 denotes the z-axis. For high values of analyte concentration, mass transport effects are negligible even at low flow rates. In (ii), however, the local analyte concentration varies due to the chemical reactions involving the analyte, thus even at high flow rates there is depletion of analyte molecules at the biomimetic surface and thus $A(x_1, x_2, x_3, t)$. Modeling of the chemical dynamics of the system in these regions follows next.

A. Reaction-Rate-Limited Detection Kinetics

In this section, the chemical kinetics in the reaction-rate-limited regime (constant analyte concentration, $A^* > 1\mu$M) are analyzed as a two time scale dynamical system. We will use singular perturbation theory (see Theorem 4.1), to approximate the time evolution of *dimer* concentration.

Defining $u = \{\Gamma,\ \Delta,\ \Pi,\ \Upsilon,\ N,\ X,\ Y,\ Z\}^T$, and $r(u(t)) = \{R_1, R_2, R_3, R_4, R_5, R_6, R_7\}^T$,where T denotes transpose and R_i are defined in (3), we can write the system of nonlinear differential equations describing the evolution of the chemical species as

$$\frac{d}{dt}(u) = Mr(u(t)) \tag{4}$$

where M is an 8×7 matrix. The left null space of the matrix M, establishes the species conservation equations which combined with the empirical fact that $\Delta(0) \gg \Upsilon(0) \geq \Gamma(0)$, lead to the approximate relation $\Upsilon \approx \Upsilon(0)$.

Analyzing the linearized version of (4) and estimating the eigenvalues with the typical parameter values for the biosensor found in [5], it is found that $|\lambda_{7,8}| \gg |\lambda_{1,2,3,4,5,6}|$. Therefore the eigenvalues associated with the species Y and Z are larger in absolute value. Thus it can be concluded that these species decay at a rate much faster than the rest and therefore it is reasonable to place these species in the "fast" group and the rest in the "slow" group.

Define, $z = \{Y, Z\}$, and $x = \{\Gamma, \Delta, \Pi, \Upsilon, N, X\}$ and let $g(x, z)$ denote the vector field of the fast variables and $f(x, z)$ the vector field of slow variables. Equations (3),(4) can be expressed as a two-time scale system;

$$\dot{x} = f(x, z) \quad \epsilon \dot{z} = g(x, z) \tag{5}$$

Here $\epsilon \approx \frac{1}{|\lambda_7|} = 10^{-2}$ is chosen as the smallest time constant of the governing differential equations [9].

The following theorem uses basic singular perturbation theory, specifically Tikhonov's theorem, [9, Sec.11.1], as well as the approximate relation, $\Upsilon \approx \Upsilon(0)$, to simplify the above two-time scale nonlinear system. The resulting simplified system yields the evolution of the conductance of the biosensor versus analyte concentration according to the two modes described in Section III-B, namely linear, and exponential decay.

Theorem 4.1: Consider the chemical species dynamics depicted by the two time scale system (5). Then as $\epsilon \to 0$, the fast time-scale variables arrive at the quasi-steady state and the dimer concentration, $\bar{\Pi}(t)$, converges to the trajectory of the following system:

$$\boxed{\frac{d}{dt}(\bar{\Pi}(t)) = -\bar{\Pi}(r_5 + f_6 A^*) + \left(f_5 \Delta + \frac{r_6 f_7 X}{r_6 + r_7}\right) \Upsilon(0)} \tag{6}$$

Specifically the trajectories that start in an $O(\epsilon)$ neighborhood of $z = h(x)$, where $h(x)$ denotes the solution of the algebraic equation $g(x, z) = 0$ satisfy

$$|\Pi(t) - \bar{\Pi}(t)| \ = \ O(\epsilon), \quad |z(t) - \bar{z}| = O(\epsilon) \tag{7}$$

for all $t \in [0, T]$ where T denotes a finite time horizon.

Eq. 6 can be solved using Euler's method with step size $h > 0$ to arrive at

$$\begin{aligned} \Pi_{n+1} = &\left(1 - (r_5 + f_6 A^*)h\right) \Pi_n + \\ &h\left(\Upsilon(0)\left(\frac{f_5 \Delta(r_6 + r_7) + r_6 f_7 X}{r_6 + r_7}\right)\right) \end{aligned} \tag{8}$$

The proof of Theorem 2.1 follows the procedure outlined in Theorem 11.1 in [9, Sec.11.1].

Therefore the *dimer* concentration of the biosensor, Π, evolves according to one of the following three modes, depending on the concentration of the analyte, A^*

$$\Pi_{n+1} = f^{\mathcal{M}}(\Pi_n, A^*) + w_n, \tag{9}$$

$$\mathcal{M} = \begin{cases} 1 & A^* = 0 : f^{\mathcal{M}}(\Pi_n, A^*) = \Pi_n \\ 2 & A^* \text{medium} : f^{\mathcal{M}}(\Pi_n, A^*) = \kappa_1 \Pi_n + \kappa_2 \\ 3 & A^* \text{high} : f^{\mathcal{M}}(\Pi_n, A^*) = \kappa_3 \Pi_n + \kappa_4 \end{cases}$$

where the constants κ_i for $i \in \{1, 2, 3, 4\}$ are calculated from the following equations using medium A^* for κ_1 and high A^* for κ_3

$$\begin{aligned} \kappa_{1,3} &= \left(1 - (r_5 + f_6 A^*)h\right), \\ \kappa_{2,4} &= h\left(\Upsilon(0)\left(\frac{f_5 \Delta(r_6 + r_7) + r_6 f_7 X}{r_6 + r_7}\right)\right) \end{aligned} \tag{10}$$

Using (9) and noting that the channel conductance is directly proportional to *dimer* concentration, we conclude that (1) describes the evolution of the channel conductance in response to variable analyte concentration.

B. Mass Transport Influenced Detection Kinetics

In this section the partial differential equation governing the dynamics of the analyte concentration, $A(x_1, x_2, x_3, t)$, which is no longer constant, is derived.

Analyte is transported to the reacting surface of the biosensor, by diffusion and flow, where it reacts with the immobilized receptors. The flow chamber has a rectangular cross section with height along the x_3-axis $h = 100\mu$m length along the x_1-axis $L = 9$mm and the width along the x_2-axis $W = 2$mm.

Due to the small aspect ration, $h/W = 0.05$, of the ICS biosensor flow chamber, the variations of analyte concentration along the x_2-axis can be ignored [1]. Therefore the analyte concentration in the flow chamber is $A(x_1, x_3, t)$ and is governed by

$$\frac{\partial A}{\partial t} = D(\frac{\partial^2 A}{\partial x_1^2} + \frac{\partial^2 A}{\partial x_3^2}) + \upsilon \frac{\partial A}{\partial x_1} \tag{11}$$

where D denotes the diffusivity of the analyte, and υ denotes the flow rate of the solution that contains the analyte.

There are four boundary conditions that need to be considered. The chamber boundary at $x_3 = h$ is reflective and the mass flux must equal zero

$$\frac{\partial A}{\partial x_3}|_{(x_1, x_3 = h, t)} = 0 \tag{12}$$

however, on the biomimetic surface at $x_3 = 0$, the mass flux must equal the time rate of change of the concentration of the species which combine with a. Therefore the analyte mass flux at $x_3 = 0$ can be defined as;

$$\frac{\partial A}{\partial x_3}|_{(x_1, x_3 = 0, t)} = -\frac{1}{D}\left(\frac{\partial X}{\partial t} + \frac{\partial N}{\partial t}\right)$$

where, $\frac{\partial X}{\partial t}$ and $\frac{\partial N}{\partial t}$ are nonlinear functions defined in (4). At the entry to the flow cell at $x_1 = 0$, the analyte concentration is equal to the injection concentration, $\bar{A}$ and at the end of the flow cell ($x_1 = L$) where the analyte exits the mass flux is zero, i.e.,

$$A(x_1 = 0, x_3, t) = \bar{A}, \qquad \frac{\partial A}{\partial x_1}|_{(x_1 = L, x_3, t)} = 0 \tag{13}$$

The analyte concentration $A(x_1, x_3, t)$ is therefore found by solving (11) subject to boundary conditions (12-13), using either finite element or finite difference methods.

Using 1nM Streptavidin with $D = 5 \times 10^{-7}\mathrm{cm}^2\mathrm{s}^{-1}$ as the protein and biotin, with concentration $7 \times 10^8 \mathrm{mol/cm}^2$, as a low molecular weight receptor, finite element method was used to simulate the chemical kinetics as well as mass transport of the analyte molecules in the biosensor with various υ values. Fig. 2 shows the plot of $\Pi(t)$ for indicated values of υ. The blue curve shows $\Pi(t)$ when mass transport is ignored. It is expected that $\Pi(t)$ for very large υ will be close to this blue curve. It is seen on Fig. 2 that, as υ is increased the chemical kinetics (red curves), approach the blue curve, i.e. the chemical kinetics are pushed into the reaction-rate limited region for which the analyte concentration is constant.

V. Conclusions

This paper began with a description of construction and operation of the ion channel biosensor. The electrical dynamics of the biosensor were modeled by a second order linear system. Furthermore, the chemical kinetics of the biosensor were modeled as a two-timescale nonlinear dynamical system in case of reaction-rate limited dynamics.

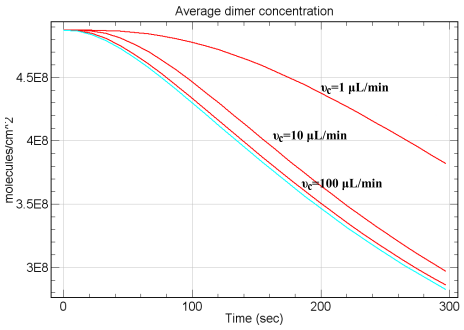

Fig. 2. $\Pi(t)$ for 1nM streptavidin as analyte and biotin with concentration $7 \times (10^8)\mathrm{mol/cm}^2$ as binding site with different flow rates, υ.

The evolution of the analyte concentration in time and space in the mass transport influenced region of operation was modeled by a partial differential equation. Using Singular Perturbation theory, analytical equations expressing the evolution of the *dimer* concentration with time as a function of analyte concentration were derived.

References

[1] J.P. Brody, P. Yager, R.E. Goldstein, and R.H. Austin. Biotechnology at low reynolds numbers. *Biophysical Journal*, 71:3430–3441, 1996.

[2] B. Cornell. *Optical biosensors: Present and future*, page 457. Elsevier, 2002.

[3] B. Cornell, V.L. Braach-Maksvytis, L.G. King, P.D. Osman, B. Raguse, L. Wieczorek, and R.J. Pace. A biosensor that uses ion-channel switches. *Nature*, 387:580–583, 1997.

[4] B. Cornell, G. Krishna, P. Osman, R. Pace, and L. Wieczorek. Tethered bilayer lipid membranes as a support for membrane-active peptides. *Biochemical Society Transactions*, 29(4):613–617, 2001.

[5] F. de Hoog and H. Huynh. Analysis of chemical reactions in the ambri membrane biosensor. Technical Report Report No. CMS-C/96/83, CSIRO dms, 1996.

[6] G.Q. Dong, L. Jakobowski, M.A.J. Iafolla, and D.R. McMillen. Simplification of stochastic chemical reaction models with fast and slow dynamics. *Journal of Biological Physics*, 33(1):67–95, Feb 2007.

[7] David A. Edwards. Estimating rate constants in a convection-diffusion system with a boundary reaction. *IMA Journal of Applied Mathematics*, 63:89–112, 1999.

[8] B. Goldstein, D. Coombs, X. He, A.R. Pineda, and C. Wofsy. The influence of trasnport on the kinetics of binding to surface receptors: application to cell and biacore. *Journal of Molecular Recognition*, 12:293–299, 1999.

[9] H.K. Khalil. *Nonlinear Systems*. Prentice Hall, 3 edition, 2002.

[10] T. Mason, A.R. Pineda, C. Wofsy, and B. Goldstein. Effective rate models for the analysis of transport-dependent biosensor data. *Mathematical Bioscience*, 159:123–144, 1999.

[11] F. Separovic and B. Cornell. Gated ion channel-based biosensor device. In S.H. Chung, O. Andersen, and V. Krishnamurthy, editors, *Biological Membrane Ion Channels*, pages 595–621. Springer-Verlag, 2007.

[12] R.A. Vijayendran, F.S. Ligler, and D.E. Leckband. A computational reaction-diffusion model for analysis of transport-limited kinetics. *Journal of Analytical Chemistry*, 71:5405–5412, 1999.

[13] G. Woodhouse, L. King, L. Wieczorek, P. Osman, and B.Cornell. The ion channel swtich biosensor. *Journal of Molecular Recognition*, 12(5), 1999.